Cell-Free Optimized Production of Protoporphyrin IX

David C. Garcia[1], John P. Davies[1], Katherine Rhea[1], Marilyn F. Lee[1], Matthew M. Lux[1*]

[1]US Army DEVCOM Chemical Biological Center, Aberdeen Proving Ground, MD, USA

KEYWORDS: Cell-free, Cell-free Metabolic Engineering, Bioproduction, Porphyrins

ABSTRACT

Background The asymmetric and aromatic structures of porphyrins enable semiconducting properties allowing them to absorb light to initiate complex photocatalytic activity. These properties coupled with biological origins have garnered these molecules and their derivatives wide interest as a biotechnological platform. However, porphyrin production in cells is challenging due to limited titers, long production timescales, and difficult purification.

Results A cell-free metabolic engineering platform was constructed to produce protoporphyrin IX (PPIX) from *E. coli* crude extracts. Using acoustic liquid-handling, design of experiments for high-throughput buffer optimization and co-culturing techniques for extract production, our cell-free reactions effectively produced 0.109 mg/mL quantities of porphyrins.

Conclusions The use of cell-free metabolic engineering as a bioproduction platform could improve the production of toxic or inefficient biomolecules such as PPIX. The engineering strategies applied in this study provide a roadmap towards increasing the scale of cell-free metabolic engineering by elucidating batch to batch variability, as well as the need for batch specific optimization of reaction conditions.

Keywords Cell-Free, Metabolic Engineering, Co-cultivation, porphyrins

Background

Porphyrins are molecules composed of one or more cyclic tetrapyrroles whose aromaticity enable semiconductor-like properties, making them useful in a broad range of applications, including artificial photosynthesis and light harvesting, catalysis, single-molecule electronics, sensors, nonlinear optics, and chemical warfare agent degradation [1–6]. Chemical syntheses and isolation of porphyrins from living cells using organic extraction or enzymatic hydrolysis is complex and poses significant challenges for scaling their

bioproduction[7–9]. The production of porphyrins in cells can be limited by a variety of factors depending on the context, including complex metabolic regulation, slow enzymatic catalysis, and post-production processing[10–12]. In the case of heme production, the cells require extensive reengineering in order to export the major product[13]. These bottlenecks in their metabolism and isolation showcase an excellent opportunity to produce porphyrins outside of the biological limitations imposed by a cell.

One potential solution to these limitations is cell-free metabolic engineering (CFME), where enzymatic pathways are reconstituted outside the cell. CFME offers an excellent opportunity to biologically produce molecules with complex metabolic pathways or difficult to implement growth regimes. Removing biological production from a cellular context offers significant advantages as toxic products, deleterious growth conditions, and even lethal metabolic states can be implemented without the need to maintain cellular viability[13,14]. Moreover, CFME can enable far higher throughput than genetic manipulation of cells. While some CFME work uses purified enzymes, here we focus on overexpressed enzymes in crude lysates due to the partially intact cellular metabolism, simpler workflow, and reduced expense. In addition, applications in healthcare settings incentivize protoporphyrin production outside of a cellular context, making cell-free production an even more attractive method for the development of medically relevant molecules[15,16].

Despite these advantages there are several limitations of CFME. For one, taking advantage of the high-throughput capacity of CFME is typically limited by slow and time-consuming chromatographic characterization methods[17,18]. Additionally, CFME extract production relies on growing and processing separate extracts for each node in a metabolic pathway and often adding expensive cofactors, significantly increasing the burden of using extracts for both prototyping and scaled production, especially for complex pathways. As a result, reported CFME efforts have so far remained at the bench instead of proceeding as a scalable biomanufacturing platform.

In this work we take advantage of porphyrins as both a molecule of interest and as an easily detectable product in a cell-free extract to i) show our ability to produce porphyrins using enriched cell-free extracts, ii) explore consolidating the extract source cells into a single co-culture fermentation in order to limit the need for multiple

extract productions, and iii) rapidly generate ideal cofactor and substrate mixtures using DBTL-cycles powered by Design of Experiments (DOE). We chose one porphyrin molecule, protoporphyrin IX (PPIX), as our target molecule due to its utility in chemical warfare agent degradation[6]. We showcase the production of PPIX in cell-free extracts and provide insights into how the production of extracts for CFME can be scaled and optimized towards cell-free biomanufacturing beyond the lab scale.

Methods

Cell-Free Extract Preparation

Cell extracts were prepared from *E. coli* BL21(DE3)pLysS cells transformed with one of seven plasmids to express PPIX synthesis pathway enzymes. All seven plasmids were assembled using a pY71 backbone expression vector containing a T7 promoter, and kanamycin resistance cassette. The *hemA* gene from *Rhodobacter capsulatus* (GenBank accession number X53309) was purchased as a gene fragment, then inserted into the PCR-linearized plasmid backbone using NEBuilder HiFi DNA assembly[6]. The sequence of the complete pY71 HemA assembly is available on GenBank (MK138544). The other six enzymes of the pathway were amplified from the *E. coli* chromosome and inserted into the same expression vector. Sequence information is provided in Supplementary Table 3. Cells were grown at 37 °C in 2xYPT (16 g L-1 tryptone, 10 g L-1 yeast extract, 5 g L-1 NaCl, 7 g L-1 KH2PO4, 3 g L-1 K2HPO4). Unless otherwise noted, cell extracts were prepared by seeding with 2.5% v/v of overnight culture and inducing with IPTG at 1 mM at an OD600 of 0.6-0.8. 200-mL or 1 L cultures were grown in 500 mL or 2 L baffled Erlenmeyer flasks, respectively. Cells were harvested by centrifugation at 5000×g for 10 min and washed with S30 buffer (14 mM magnesium acetate, 60 mM potassium acetate, and 10 mM Tris-acetate, pH 8.2) by resuspension and centrifugation. The pellets were weighed, flash-frozen, and stored at −80 °C. Extracts were prepared by thawing and resuspending the cells in 0.8 mL of S30 buffer per gram of cell wet weight. The resuspension was lysed using 530 J per mL of suspension at 50% tip amplitude with ice water cooling. Homogenization was performed as described previously using a Microfluidizer (Microfluidics M-110P) on a cell suspension (prepared the same as the sonication protocol)

using one pass followed by centrifugation[19]. Following sonication or homogenization, tubes of cell extract were centrifuged twice at 21,100×g for 10 min at 4 °C, aliquoted, frozen with liquid nitrogen, and stored at −80 °C.

CFME Reaction Set-up

PPIX production reactions were carried out at 37°C in 4 µL volumes without shaking. Unless otherwise noted, each reaction contained 2.5 mM succinate, 1.25 mM Acetyl-CoA, 1.25 mM ATP, 18.76 mM glycine, and 10 mM Pyridoxal 5′-phosphate. Unless otherwise noted extracts were added to a final protein concentration of 13.5 mg/mL as measured by Bradford assay. Reaction components were directly dispensed into a clear-bottom-384 well plate using an Echo 525 Liquid Handler (Beckman Coulter).

Analysis and Quantification of Porphyrins

PPIX levels were quantified using a standard curve method using synthesized PPIX standard purchased from Frontier Scientific Inc. (Logan, UT, USA, P562-9), read with a Synergy Neo2 Multi-Mode Microplate Reader (Biotek) set to an excitation and emission of 410 and 633 nm, respectively. Plate reader experiments were performed using 384-well assay plate (Corning, Kennebunk, ME, 04034, USA) covered with a plate sealer (Thermo Scientific, Rochester, NY, 14625, USA) HPLC analysis was performed using Agilent 1290 Infinity II equipped with a diode array detector (DAD) reading at 410 nm and a BDS Hypersil C18 column 150 × 2.1 mM, 2.4 µm particle size (Thermo Scientific, Waltham, MA, USA, 28102–152130). A mobile phase of A: 0.1% formic acid in ultrapure water, and solvent B: 0.1% formic acid in methanol was used at a flow rate of 0.4 mL/min. Injections of 20 µL were separated by a linear gradient transitioning from 100% solvent A to 100% solvent B over 20 min, followed by 100% B solvent for 10 minutes.

DOE and Statistical Analysis

DOE designs and models were prepared using Stat-Ease Design-Expert 13 and SAS JMP® Pro 15. DOE data analysis was performed using Functional Data Analysis (FDA) applied via the “Functional Data Explorer” platform within SAS JMP® Pro 15 software[20]. A Functional Principal Components (FPC) decomposition was then applied to the response curves. Optimized reaction conditions were found via the Stat-Ease Design-Expert

13 Numerical Optimization feature SAS JMP® Pro 15 software Prediction Profiler Platform. Further data analysis and plots were prepared using custom python scripts.

Results

PPIX production using individually enriched extracts

The previously-characterized C4 pathway examined here involves seven enzymes for over-production of PPIX (HemA-G) and starts with a condensation of glycine and succinyl CoA **(Figure 1A)**[21]. Our initial experiments were performed by heterologously overexpressing each of these enzymes from plasmids in separate *E. coli* cultures and lysing the cells to produce extracts enriched with enzymes for each step in the PPIX pathway, referred to as individually enriched extracts for the rest of the manuscript (**Figure 1B)**. CFME reactions were assembled by combining individually enriched extracts with substrates and cofactors to reactivate the complete pathway outside of the cell. The reaction mixtures contain ATP, Succinate, Glycine, Pyridoxal 5′-phosphate (P5P), and Coenzyme A (CoA) and were incubated at 37°C. Importantly, we found that the CFME reactions expressing HemA-F and HemA-G both showed measurable amounts of a porphyrin that was identified as PPIX by HPLC compared to porphyrin standards. However, the concentration considerably decreased in the absence of HemF indicating its importance towards producing PPIX (**Supplemental Figure 1A-B)**. Towards rapid optimization of this pathway, all further experiments were measured using plate reader fluorescence measurements of the entire CFME reaction (EX410nm/EM:633nm) and quantified by standard curve (**Supplemental Figure 1C-D)**. Though the upstream products of PPIX also fluoresce at these wavelengths, the single PPIX peak in the chromatograms supported the assumption that the fluorescence signal was largely derived from PPIX for the purposes of rapid screening. Individually enriched extracts were mixed in several different combinations and the relative levels of extracts were varied to reveal trends in the production of PPIX fluorescence (**Figure 1B)**. None of the individual extracts produced high protoporphyrin levels on their own, yet leave-one-out mixtures of the full set still resulted in some PPIX being produced for some enzymes. This observation indicates that some endogenous PPIX pathway enzymes were active in the *E.*

coli lysates, though the amount of PPIX produced was much less than reactions where all seven enriched extracts were combined[21].

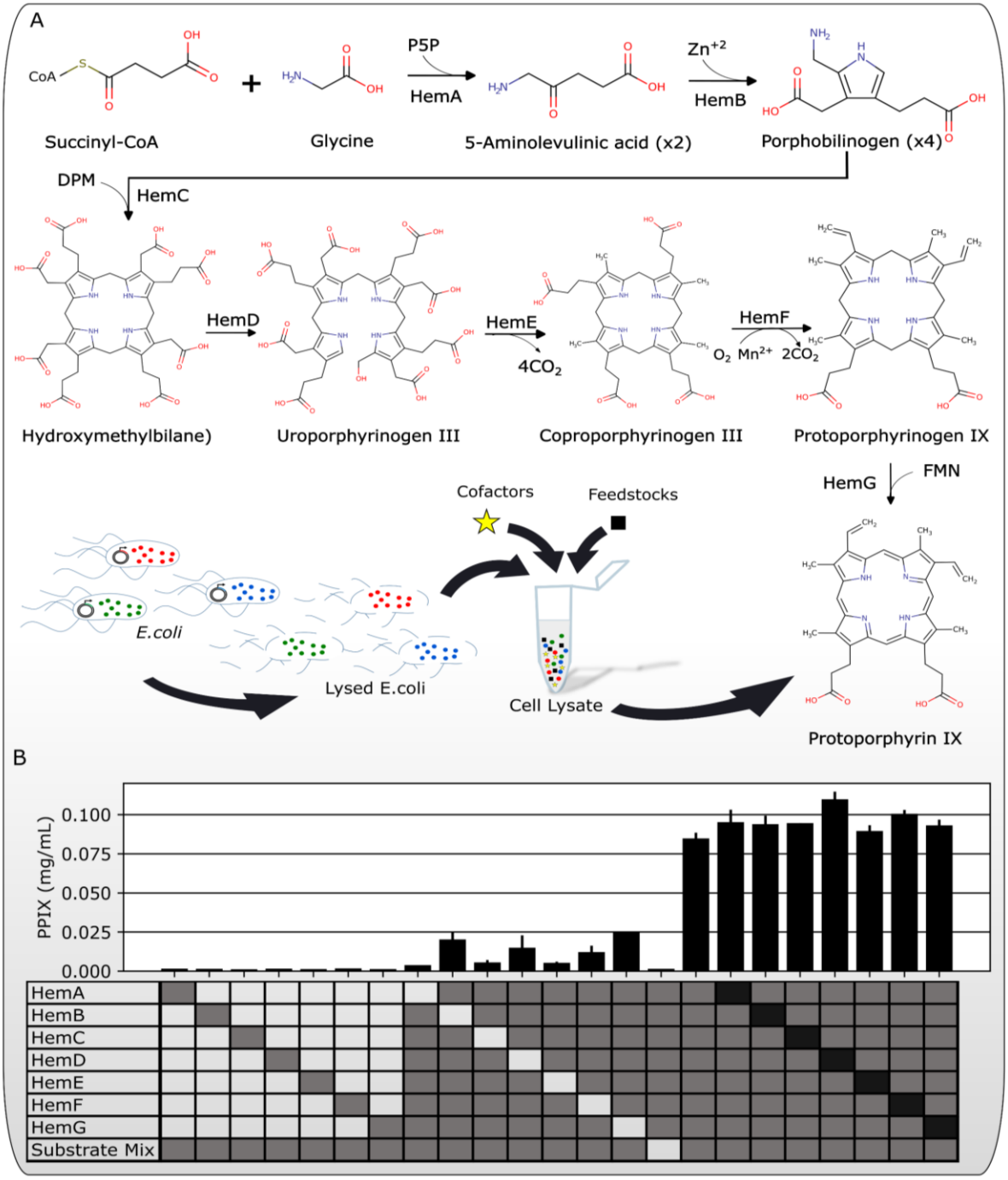

Figure 1. Production of PPIX with CFME. **A.** The C4 pathway for biosynthesis of PPIX. **B.** The full metabolic pathway is reconstituted in cell-free extracts by overexpressing individual enzymes in separate *E. coli* strains and combining enriched extracts in various combinations and relative levels to produce PPIX as measured by fluorescence (EX410nm/EM:633nm).

An empty square indicates the absence of the reagent and black indicates double the concentration. Data for bar plots were acquired using n ≥ 3 biological replicates. Error bars represent standard deviation of the replicates.

A co-culture approach to produce CFME extracts

Since the labor and cost of producing individually enriched extracts is directly proportional to the number of nodes in the metabolic pathway of interest, producing CFME materials for complex pathways can become laborious. While cell-free protein synthesis can be used to produce the enzymes for CFME post-extraction, the reactions are generally more productive if the enzymes are pre-enriched in the cells prior to extract preparation[22,23]. We decided to explore if it was possible to simplify the extract preparation process by growing all of the source strains, each expressing only one enzyme, in a co-culture within the same flask, thus allowing for a single fermentation to generate the full metabolic pathway (**Figure 2A)**. In this scheme, the pathway is optimized with a high degree of control using individual enriched extracts, followed by using a pooled inoculation to scale reactions in a single fermentation.

Our first attempt to reduce the number of fermentations required to produce an active CFME pathway used a base co-culture extract grown from equal inoculations of each of the 7 strains expressing nodes in the PPIX pathway, termed Hem(AG) to indicate the enzymes coming from the same culture and extraction. This first co-culture lysate had low detected production of PPIX. To troubleshoot, the co-culture Hem(AG) extract was supplemented with an extract of each of the individually expressed nodes (Hem(AG)+HemA, etc.) **(Figure 2B)**. Supplementing several of the extracts enriched with single enzymes increased the amount of PPIX produced from the base extract. HemA, the only enzyme not endogenously expressed in *E. coli,* had the greatest effect. These results suggest that some strains are being outcompeted in the co-culture, highlighting the limitations of removing the more fine-tuned control possible with reactions built from the individually enriched extracts. To combat this issue, we sought to tune growth by increasing the inoculum of strains expressing each node in the pathway. We prepared CFME extracts as before, but with doubled inoculums of each strain in turn. We found that the extracts with increased inoculations of HemB, HemC and HemG had improved final protoporphyrin yield (**Figure 2C)**. However, differences between replicates of the equal inoculum Hem(AG) experiment and

inconsistent trends from supplementation of individually enriched extracts and altering inoculum ratios pointed to more complex factors impacting observed production from co-culture exracts.

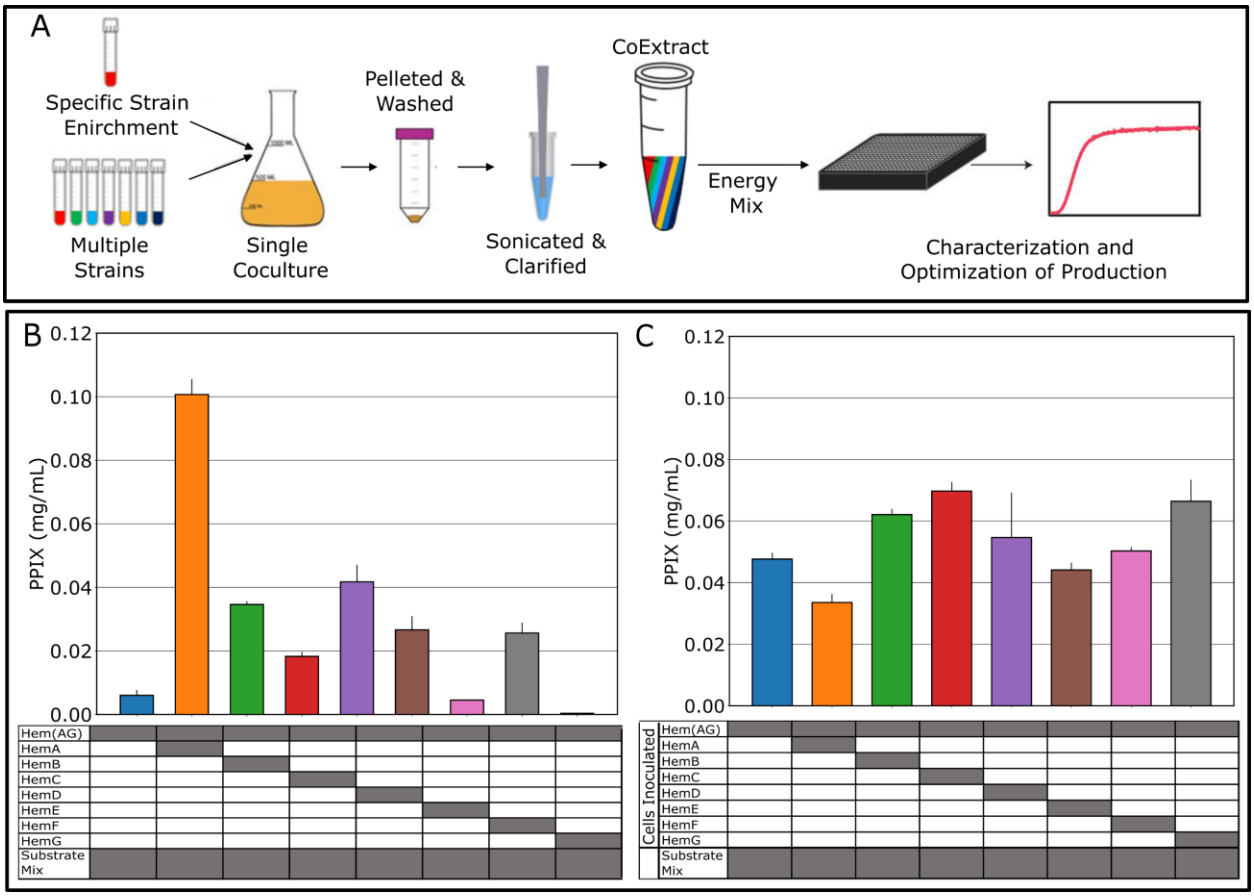

Figure 2. **A.** Cell-free metabolic engineering extract production strategy relying on a single co-culture consisting of all of the strains in the pathway with increased inoculations of lynchpin enzymes. **B.** Productivity of PPIX in CFME reactions created using a base co-culture extract derived from equal inoculation of strains each expressing one enzyme, HemA-G. The base extract was used at a concentration of 13.5 mg/mL total protein and additional reactions were supplemented with 1 µL individually enriched extract for each pathway enzyme. **C.** Productivity of PPIX in CFME reactions made with co-cultured cell extracts (Hem(AG)) expressing HemA-G, one enzyme expressed per co-cultured strain, with double inoculation of one strain and equal inoculation of all others.

To further explore the factors contributing to observed differences in production, we performed additional replicates of the equal inoculum Hem(AG) case and tested modifying the growth protocol, resulting in substantial batch-to-batch variability (**Supplemental Figure 2**). We attribute this variability to a complex

relationship between small variations in inocula that are amplified by exponential growth, growth competition, and burden elicited by heterologous protein production at induction. Moreover, since the proteome[24,25] and metabolic state of the extracts are influenced by the growth state of the cells at harvest, the mixed states of the different strains likely influences CFME reaction productivity in complex, unknown ways. Though activity in a co-cultured Hem(AG) extract can be tuned by supplementation with individually enriched extracts, resolving batch-to-batch variation will likely require methods of regulating growth to produce a consistent co-culture extract. This point is further evidenced by the variability in growth dynamics seen for each of the cells with and without induction. The presence of IPTG significantly impairs the growth of several of the strains, particularly cells carrying the plasmid for HemF, and elicits a general burden on the cells that causes variability within replicates (**Supplemental Figure 3**). Though less common in cell-free metabolic engineering applications, batch-to-batch variability in cell-free extracts has been explored as a factor impacting cell-free protein synthesis[26–28]. Strategies to control the dynamics of cell populations use tools like auxotrophies, or lysis circuits, but impart a further burden on the cells that may limit their bioproduction relevance[29,30].

Tuning substrate and co-factor concentrations

Despite the need for improved control for reproducibility in co-cultured CFME extracts, promising product titers incentivized us to further characterize and optimize these combined reactions. The Hem(AG) co-culture extract prepared with a double inoculation of HemC, termed Hem(AG-2xC) for the remainder of this work, was used to further explore the effects of optimizing concentrations of CFME ingredients and scaling lysate preparation. The levels of each fed substrate and cofactor can greatly impact productivity, and some of these molecules represent substantial portions of the cost of the CFME reaction (**Supplemental Table 1**). We performed a set of titrations for each of the components, starting with a Hem(AG-2xC) extract prepared from a 0.2 L shake flask culture volume. The control reaction uses 2.5 mM succinate, 1.25 mM CoA, 1.25 mM ATP, 18.76 mM glycine, and 10 mM P5P. Large changes in PPIX bioproduction occurred when modifying the mixtures and results indicated that for this 0.2 L scale lysate, the CoA, glycine, and P5P were all essential to the function of the system (**Figure 3A**). Interestingly, while the yield of PPIX from 37.5 mM glycine was only 2.39%, the overall PPIX titer of reactions reached 0.063 mg/mL, comparable with previous efforts producing a similar product (up to 0.240 mg/mL of heme produced in fed batch engineered *E. coli* cultures)[10]. The observed yield likely

draws from the background metabolism still active in the extract[29,30]. With respect to cost reduction, CoA, ATP, and P5P are the most expensive reagents **(Supplemental Table 1).** The results showed that ATP could be removed completely to decrease cost without dramatically reducing yields; CoA was required but could possibly be reduced without loss of yield; and P5P concentration increased yield, contrary to cost reduction goals.

Little has been published to date on how CFME reactions perform across scales. To begin to address this knowledge gap, we explored how larger culture volumes would impact the production of CFME lysate and the resulting PPIX product titers. We examined the PPIX productivity of a CFME extract produced from 0.2 and 3 L flask fermentations. In addition to culture volume differences, the 3 L extracts were lysed using a microfluidizer while the 0.2 L culture was processed by sonication. The 0.2 L cultures regularly reach a final OD600 of 5-8, but the 3 L fermentation only reached a final OD600 of ~3.0. We found that each lysate gave a substantially different PPIX yield using the same energy mixture with higher culture-volume extract reaching 28% of the titer of the 0.2 L fermentation (**Figure 3B)**. Given our prior findings with respect to reproducibility in co-cultured extracts even for the same conditions, we cannot attribute any observed differences specifically to the scale of the culture.

We next evaluated the substrate and cofactor dependence of CFME reactions derived from the 3 L culture. Given that prior results from a 0.2 L extract in Figure 2D showed limited dependence on ATP and the possibility to reduce CoA concentrations, we titrated these components. We found no clear dependence on either component over the ranges tested for the 3L lysate (**Figure 3C)**. Interested in this observation, we further titrated the concentration of CoA compared to succinate, finding that neither was essential in the presence of the other for the reaction to function (**Figure 3D)**. This implied that a cofactor pool was still present. Succinate and CoA could produce the essential precursor, succinyl CoA, through independent pathways, the former by completing a loop through the TCA-cycle and the latter by serving as co-factor in a number of reactions that produce succinyl-CoA. CoA was essential in CFME reactions prepared from 0.2 L scale cultures that reached a higher OD perhaps because cofactors like CoA are depleted at higher OD. Previous work has shown that cofactor pools are significantly different depending on the growth stage of the culture, with cofactor levels depleting heavily

over time[31,32]. Though not explicitly measuring cofactors, further evidence that varying growth conditions substantially impacted the metabolism and proteome of a cell-extract was shown with changes to the media and the OD at harvest[33].

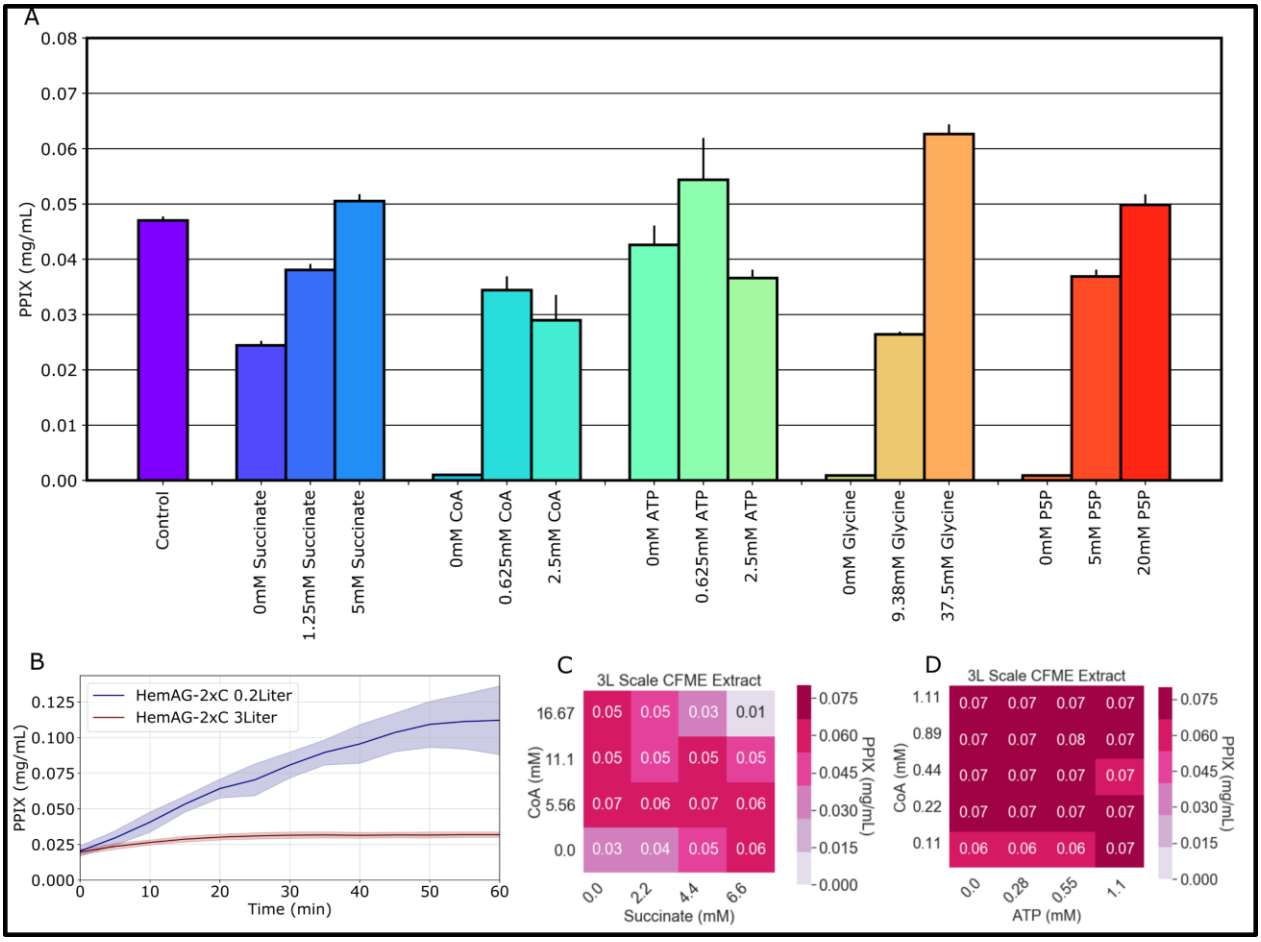

Figure 3. **A.** PPIX production following a cofactor titration in a CFME extract with a double inoculation of HemC. Data for plots were acquired using n ≥ 3 biological replicates. Error bars represent standard deviation of the replicate. B**.** PPIX production following a cofactor titration in a CFME extract with a double inoculation of HemC. Data for plots were acquired using n ≥ 3 biological replicates. Error bars represent standard deviation of the replicates. C. Heatmap of PPIX productivity from 3L-scale extract with titrations of cofactors CoA and succinate. D. Heatmap of PPIX productivity from 3L-scale extract with titrations of reduced concentrations of CoA and ATP supplements.

A DOE approach to rapid productivity and cost optimization

Since there are so many factors to explore in the design of CFME reactions, we decided to apply a Design of Experiments (DOE) approach to more quickly find optima and identify trends in the search space using a design-build-test-learn (DBTL) cycle (**Figure 4A)**. Design of Experiments (DOE) is a statistical multifactorial approach to both design and analyze an experimental process. DOE experiments modify a number of factors simultaneously and measure the resultant effect on the system. DOE provides an excellent tool to rapidly define the ideal reaction compositions and develop robust and economical cell-free bioproduction platforms.

We aimed to maximize the amount of PPIX produced using the 3 L scaled-CFME extract by creating an initial exploratory model modifying the relevant cofactors and substrates, specifically succinate, CoA, ATP, Glycine, and P5P, to produce a predictive model of the interactions. An I-optimal design composed of 300 experiments capable of estimating linear blending effects and non-linear blending effects between the substrates and cofactors produced several combinations capable of activating PPIX production (**Figure 4B**). To validate the DOE model, we picked 10 predicted optimal reaction conditions using two objective functions (**Figure 4C**). The first objective function was set to maximize the production of PPIX (mg/mL) while the second was set to maximize production at the lowest cost ($/mg) (**Supplemental Table 2**). All the predicted optimal reactions yielded final titers greater than 0.03 mg/mL aside from 4 of the cost-optimized reactions that had no PPIX production. Both models showed that Glycine and P5P were overwhelmingly the most important reagents. Interestingly, in both cases the need for CoA was removed without much change to the overall yield of the reaction. As has previously been noted, changes in growth conditions can have significant impacts on the proteome and resultant metabolome of a cell lysate[13,33]. Additionally, draining cofactor pools could have a substantial effect on the overall function of the extract and indicate why cofactors with large internal pools earlier in the growth, such as CoA would not need to be supplemented[31]. Overall, the highest titer presented in this work of 0.109 mg/mL resulted in a cost of $14.26/mg. The application of the DOE reduced the cost by about

90% with the best reaction reaching a cost of $1.41/mg, though a lower titer (0.049 mg/mL) was reached (**Supplemental Table 2**).

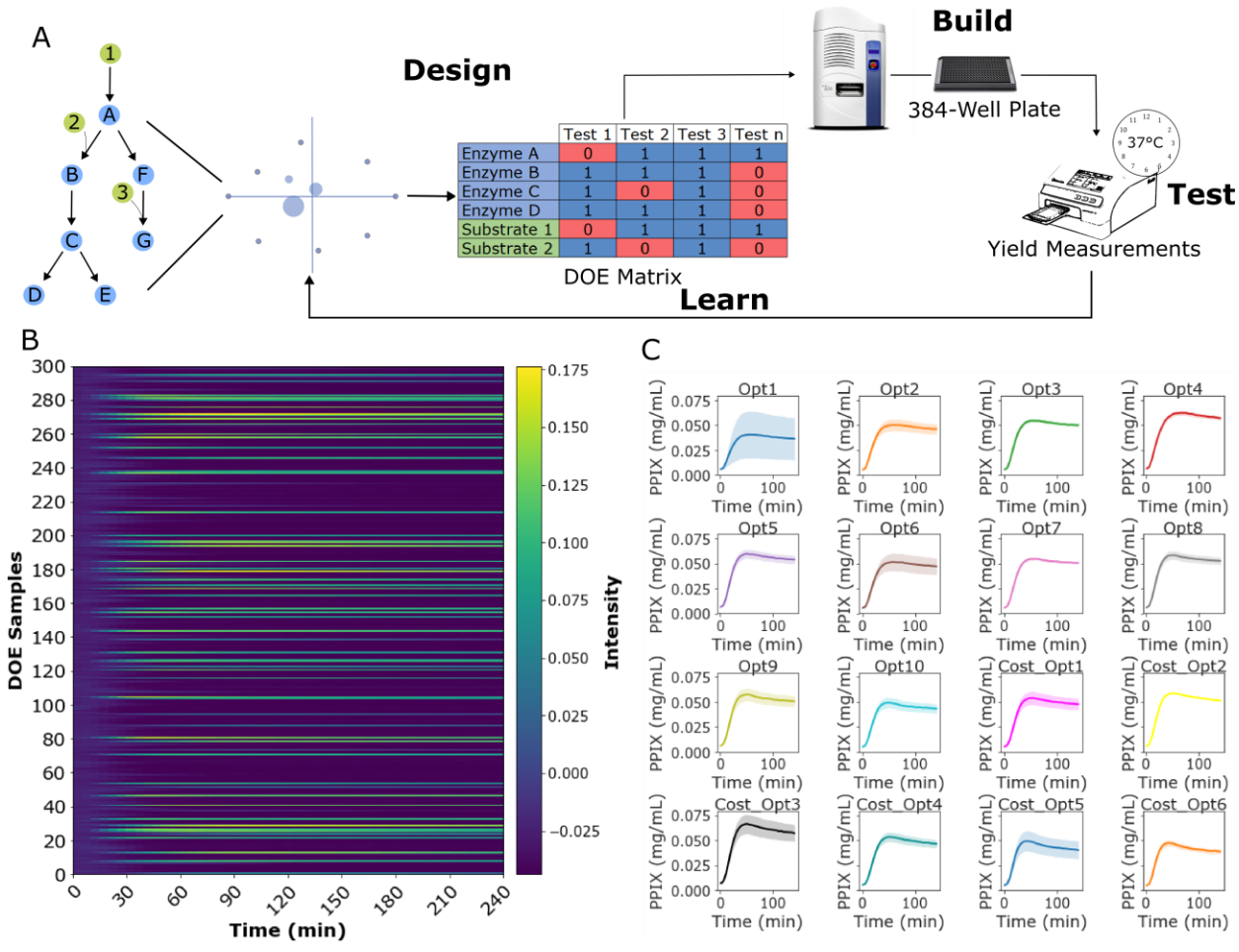

Figure 4. A. Graphic illustration of the DBTL cycle used to explore the combinatorial space of CFME compositions. Initial tests of cofactors and substrates defined an initial DOE matrix that was tested, and the resulting data used to define a predictive model for active and optimal reagent concentrations. **B.** 300-experiment DOE heatmap of PPIX produced from the addition of varied cofactors to a HemAG(2xC) CFME extract. **C.** Predicted optimal mixtures for both performance and cost were measured for fluorescence.

Conclusions

As CFME systems are implemented to produce an expanding range of molecules, an understanding of the underlying mechanisms that control their productivity will need to expand in kind. In this study, the seven-member PPIX synthesis pathway was explored, both to improve the prospects of bioproduction for this

interesting molecule, and to uncover factors with the greatest impact on CFME productivity. To start, the ability to produce PPIX in a CFME reaction was confirmed by mixing seven individually enriched extracts for each enzyme in the pathway. Following successful identification of the product, we pursued two approaches to improve productivity and reduce cost. The first approach examined a co-culture method to produce a multi-strain CFME extract with a single fermentation. We found that co-culture cell-extracts produced PPIX and titers could be increased by supplementing individually enriched extracts post-lysis or increasing inoculums of specific strains in the co-culture. Though removing substantial amounts of labor as fewer fermentations are required, very high levels of variability both in the growth of the individual strains and the resultant product titers incentivize further process improvements to maintain stable communities such as using antibiotics during growth, engineering auxotrophies to limit loss of community members, and chromosomal integration to reduce burden on the cell.

The second approach established that a larger fermentation volume also produced PPIX, but the effects of culture volume could not be disentangled from co-culture variability. Nonetheless, to show that a given extract preparation could be improved, we applied a high throughput DOE DBTL cycle to the optimization of the cofactors and substrates required for the reaction. We saw that the DOE model could accurately predict formulations with improved productivity or lower cost per yield. Importantly in the context of a manufacturing process, the DBTL cycle can easily be performed in less than 24-hours. Though the reactions from the 3-liter extract did not reach the same titer as those assembled with individually expressed-enzyme extracts, the final cost of each reaction was substantially lower both in terms of reagents and labor as only a single extract needed to be prepared compared to the 7 required for the highest yield seen in this work. These results shed light on challenges to control both enzyme and small molecule content in different lysate preparations for CFME, yet at the same time show how direct supplementation of additives allow for rapid optimization to partially compensate for variability.

The work demonstrated here establishes the foundation for a fuller understanding of the principles that underpin CFME as a biomanufacturing technology. We expect that future work will significantly expand on our efforts by limiting culturing variability and directly correlating in-depth metabolic and proteomic analysis to

the resultant productivity phenotype of the extract[34,35]. These efforts, together with engineered chassis designed to increase fluxes, improved reaction conditions, and DBTL cycles to optimize reaction formulas, will enable cell-free bioproduction strains to be optimized to meet the technical and economic benchmarks for industrial biomanufacturing.

Supplementary Information

Author's Contribution

DG, MFL, and MWL, designed the study; DG and JD carried out the experiments; KR aided with extract production; DG, MFL, and MWL wrote the manuscript; MFL and MWL supervised the study and secured the funding. All authors read and approved the final manuscript.

Funding

Funding was provided by congressional program Cell-free Biomanufacturing. This project was supported in part by an appointment to the NRC Research Associateship Program at DEVCOM Chemical Biological Center for DCG administered by the Fellowships Office of the National Academies of Sciences, Engineering, and Medicine.

Data Availability

The datasets used and/or analysed during the current study are available from the corresponding author on reasonable request.

Declarations

Ethics approval and consent to participate.

Not Applicable.

Consent for publication

Not Applicable

Competing interests

The authors declare that they have no competing interests.

Author details

[1]US Army DEVCOM Chemical Biological Center, Aberdeen Proving Ground, MD, USA

References

1. So, M. C., Wiederrecht, G. P., Mondloch, J. E., Hupp, J. T. & Farha, O. K. Metal–organic framework materials for light-harvesting and energy transfer. *Chem. Commun.* **51**, 3501–3510 (2015).
2. Zhao, M., Ou, S. & Wu, C.-D. Porous Metal–Organic Frameworks for Heterogeneous Biomimetic Catalysis. *Acc. Chem. Res.* **47**, 1199–1207 (2014).
3. Zwick, P., Dulić, D., van der Zant, H. S. J. & Mayor, M. Porphyrins as building blocks for single-molecule devices. *Nanoscale* **13**, 15500–15525 (2021).
4. Ling, P., Lei, J., Zhang, L. & Ju, H. Porphyrin-Encapsulated Metal–Organic Frameworks as Mimetic Catalysts for Electrochemical DNA Sensing via Allosteric Switch of Hairpin DNA. *Anal. Chem.* **87**, 3957–3963 (2015).
5. Yang, C.-C., Li, L., Tian, W. Q., Li, W.-Q. & Yang, L. Strong second order nonlinear optical properties of azulene-based porphyrin derivatives. *Phys. Chem. Chem. Phys.* **24**, 13275–13285 (2022).

6. Lee, M. S., Garibay, S. J., Ploskonka, A. M. & DeCoste, J. B. Bioderived protoporphyrin IX incorporation into a metal-organic framework for enhanced photocatalytic degradation of chemical warfare agents. *MRS Commun.* **9**, 464–473 (2019).
7. Espinas, N. A., Kobayashi, K., Takahashi, S., Mochizuki, N. & Masuda, T. Evaluation of Unbound Free Heme in Plant Cells by Differential Acetone Extraction. *Plant Cell Physiol.* **53**, 1344–1354 (2012).
8. In, M.-J., Kim, D. C., Chae, H. J. & Oh, N.-S. Effects of Degree of Hydrolysis and pH on the Solubility of Heme-iron Enriched Peptide in Hemoglobin Hydrolysate. *Biosci. Biotechnol. Biochem.* **67**, 365–367 (2003).
9. Martin, P., Müller, M., Flubacher, D., Boudier, A. & Spielvogel, D. Total Synthesis of Hematoporphyrin and Protoporphyrin; a Conceptually New Approach. *CHIMIA* **67**, 204 (2013).
10. Zhao, X. R., Choi, K. R. & Lee, S. Y. Metabolic engineering of Escherichia coli for secretory production of free haem. *Nat. Catal.* **1**, 720–728 (2018).
11. Kang, Z. *et al.* Recent advances in microbial production of δ-aminolevulinic acid and vitamin B12. *Biotechnol. Adv.* **30**, 1533–1542 (2012).
12. Layer, G. Heme biosynthesis in prokaryotes. *Biochim. Biophys. Acta BBA - Mol. Cell Res.* **1868**, 118861 (2021).
13. Garcia, D. C. *et al.* A lysate proteome engineering strategy for enhancing cell-free metabolite production. *Metab. Eng. Commun.* **12**, e00162 (2021).
14. Dudley, Q. M., Karim, A. S. & Jewett, M. C. Cell-free metabolic engineering: Biomanufacturing beyond the cell. *Biotechnol. J.* **10**, 69–82 (2015).
15. Yoshioka, E. *et al.* Enhancement of Cancer-Specific Protoporphyrin IX Fluorescence by Targeting Oncogenic Ras/MEK Pathway. *Theranostics* **8**, 2134–2146 (2018).
16. Hirai, K., Sasahira, T., Ohmori, H., Fujii, K. & Kuniyasu, H. Inhibition of heme oxygenase-1 by zinc protoporphyrin IX reduces tumor growth of LL/2 lung cancer in C57BL mice. *Int. J. Cancer* **120**, 500–505 (2007).
17. Kay, J. E. & Jewett, M. C. Lysate of engineered Escherichia coli supports high-level conversion of glucose to 2,3-butanediol. *Metab. Eng.* **32**, 133–142 (2015).
18. Korman, T. P., Opgenorth, P. H. & Bowie, J. U. A synthetic biochemistry platform for cell free production of monoterpenes from glucose. *Nat. Commun.* **8**, 15526 (2017).

19. Lee, M. S. *et al. Cell-Free Protein Expression in Polymer Materials*. http://biorxiv.org/lookup/doi/10.1101/2023.08.18.553881 (2023) doi:10.1101/2023.08.18.553881.

20. Gilman, J., Walls, L., Bandiera, L. & Menolascina, F. Statistical Design of Experiments for Synthetic Biology. *ACS Synth. Biol.* **10**, 1–18 (2021).

21. Turlin, E. *et al.* Protoporphyrin (PPIX) efflux by the MacAB-TolC pump in *Escherichia coli*. *MicrobiologyOpen* **3**, 849–859 (2014).

22. Karim, A. S. & Jewett, M. C. A cell-free framework for rapid biosynthetic pathway prototyping and enzyme discovery. *Metab. Eng.* **36**, 116–126 (2016).

23. Karim, A. S. & Jewett, M. C. Cell-Free Synthetic Biology for Pathway Prototyping. in *Methods in Enzymology* vol. 608 31–57 (Elsevier, 2018).

24. Falgenhauer, E. *et al.* Evaluation of an *E. coli* Cell Extract Prepared by Lysozyme-Assisted Sonication via Gene Expression, Phage Assembly and Proteomics. *ChemBioChem* **22**, 2805–2813 (2021).

25. Failmezger, J., Rauter, M., Nitschel, R., Kraml, M. & Siemann-Herzberg, M. Cell-free protein synthesis from non-growing, stressed Escherichia coli. *Sci. Rep.* **7**, 16524 (2017).

26. Dinglasan, J. L. N. & Doktycz, M. J. Rewiring cell-free metabolic flux in *E. coli* lysates using a block—push—pull approach. *Synth. Biol.* **8**, ysad007 (2023).

27. Hunter, D. J. B., Bhumkar, A., Giles, N., Sierecki, E. & Gambin, Y. Unexpected instabilities explain batch-to-batch variability in cell-free protein expression systems. *Biotechnol. Bioeng.* **115**, 1904–1914 (2018).

28. Dopp, J. L., Jo, Y. R. & Reuel, N. F. Methods to reduce variability in E. Coli-based cell-free protein expression experiments. *Synth. Syst. Biotechnol.* **4**, 204–211 (2019).

29. Mee, M. T., Collins, J. J., Church, G. M. & Wang, H. H. Syntrophic exchange in synthetic microbial communities. *Proc. Natl. Acad. Sci.* **111**, (2014).

30. Hsu, C.-Y., Yu, T.-C., Lin, L.-J., Hu, R.-H. & Chen, B.-S. Systematic approach to Escherichia coli cell population control using a genetic lysis circuit. *BMC Syst. Biol.* **8**, S7 (2014).

31. Vadali, R. Cofactor engineering of intracellular CoA/acetyl-CoA and its effect on metabolic flux redistribution in Escherichia coli. *Metab. Eng.* **6**, 133–139 (2004).

32. Leonardi, R. & Jackowski, S. Biosynthesis of Pantothenic Acid and Coenzyme A. *EcoSal Plus* **2**, ecosalplus.3.6.3.4 (2007).

401 33.Garcia, D. C. *et al.* Elucidating the potential of crude cell extracts for producing pyruvate from glucose. *Synth.*
402 *Biol.* **3**, ysy006 (2018).
403 34.Contreras-Llano, L. E. *et al.* Holistic engineering of cell-free systems through proteome-reprogramming
404 synthetic circuits. *Nat. Commun.* **11**, 3138 (2020).
405 35.Hurst, G. B. *et al.* Proteomics-Based Tools for Evaluation of Cell-Free Protein Synthesis. *Anal. Chem.* **89**,
406 11443–11451 (2017).
407

Supplemental Figures

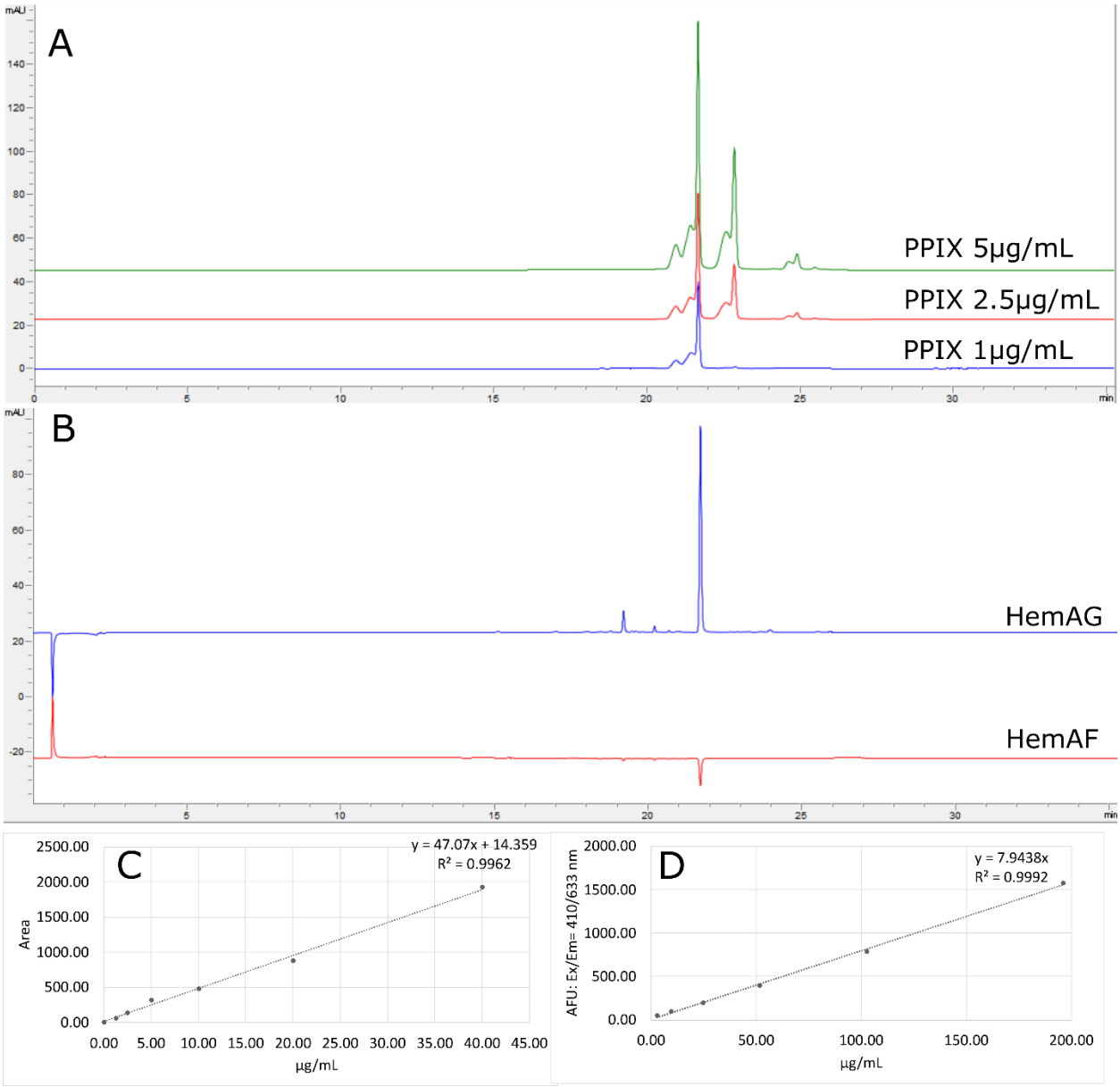

Supplemental Figure 1. Representative chromatograms of PPIX standards and CFME samples. A. A peak is seen for purified PPIX at 21.6 minutes. B. The same peak is seen at 21.6 minutes when the complete pathway is present in a CFME reaction, but nearly disappears when the last enzyme in the pathway is absent. A small amount of PPIX is detectable as expected without HemG as E. coli naturally produces the enzyme, but not in sufficient quantities to be noticeable by fluorescence measurements. C. PPIX standard curve produced using purified reagent. D. PPIX producing cell-free samples measured with a plate reader, extracted, and cross-referenced to the purified PPIX curve.

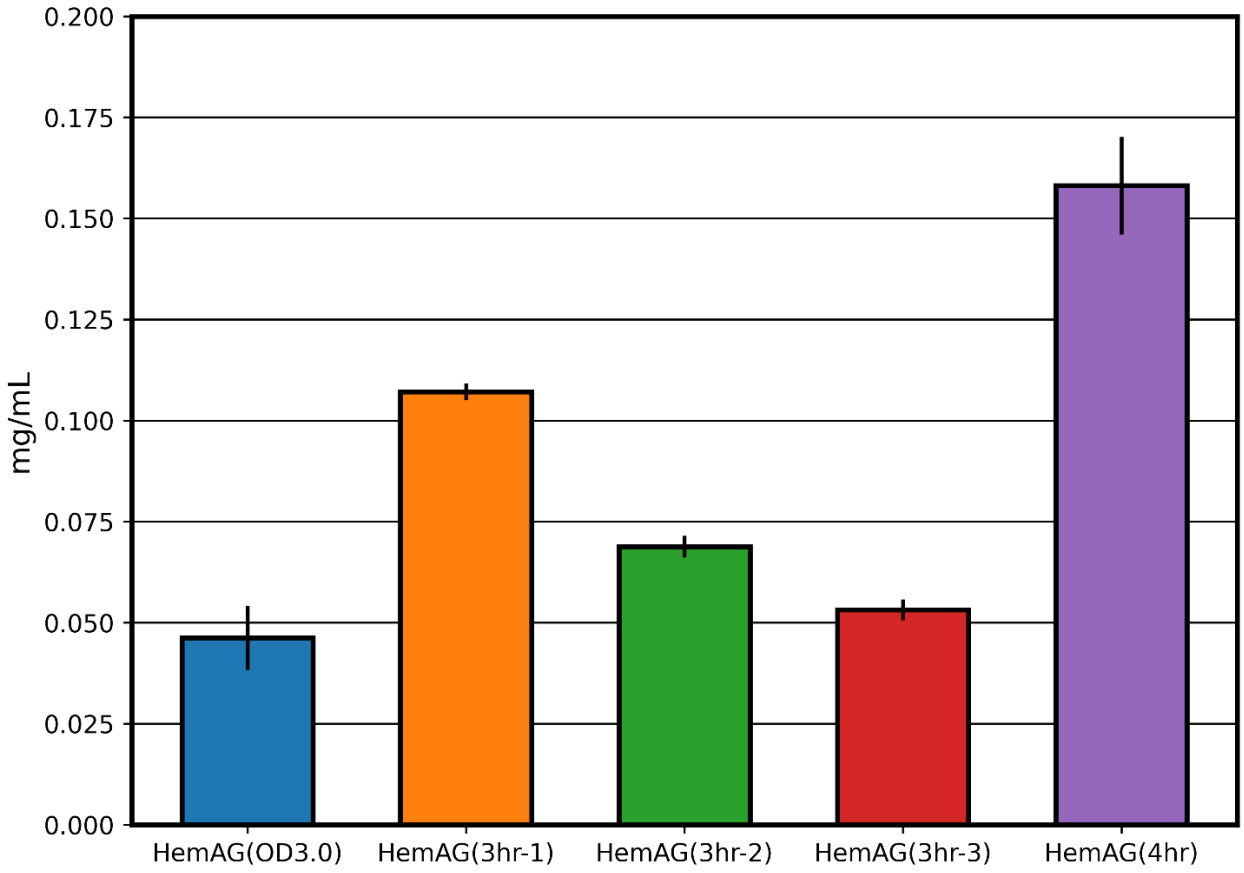

Supplemental Figure 2. PPIX-producing enriched extracts were prepared using the same inoculation conditions. Following induction with 1mM IPTG, the cells were allowed to grow at 30° C for varying amounts of time or until a specific OD600 as noted in the legend. The CFME reactions were prepared using the conditions noted in the methods and reported from .

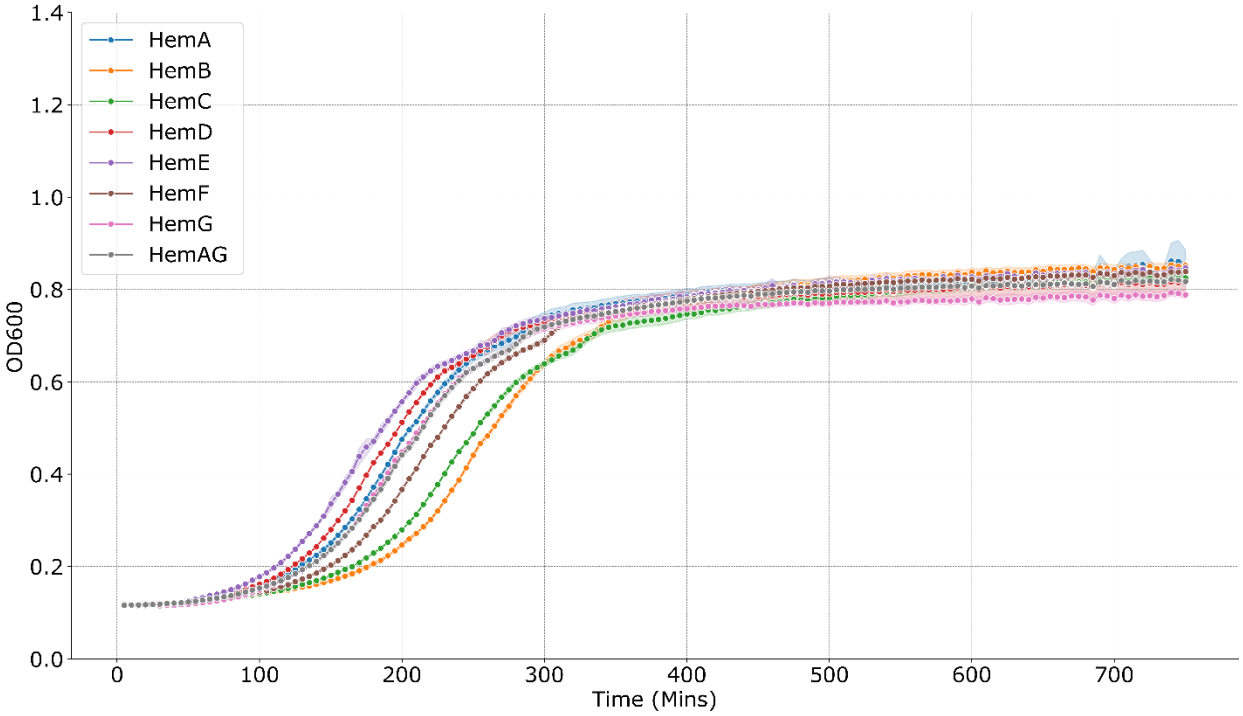

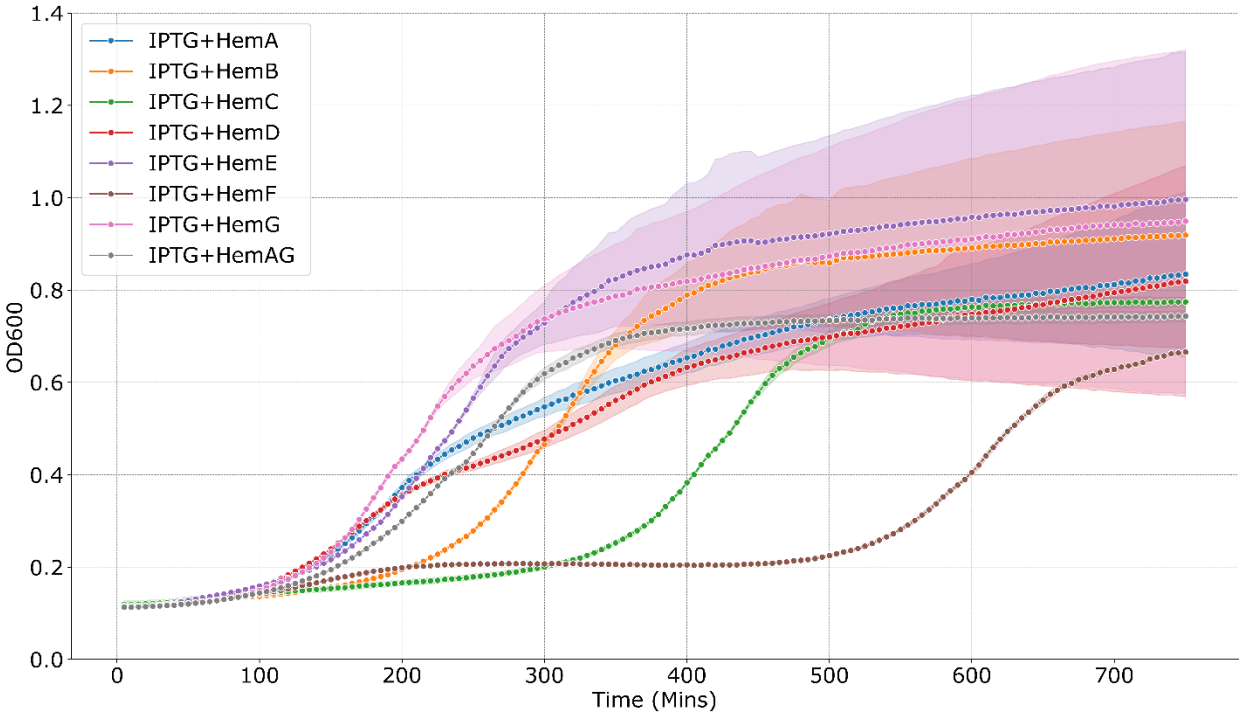

421

422 **Supplemental Figure 3.** Growth curves of *E. coli* cells expressing PPIX pathway enzymes individually and combined in

423 2xYPT medium with no antibiotics. **Top:** Cells were inoculated without the presence of IPTG. **Lower**: Cells were inoculated

with 1mM IPTG at t=0. Data for line plots were acquired using n ≥ 4 biological replicates. Error bars represent standard deviation of the replicates.

Supplemental Table 1: Reagent costs for cofactors and substrates. Cost based on Sigma Aldrich Checked

Reagent	MW	Cost/L($)
Succinate(100 mM)	118.09	0.21
Glycine(500 mM)	75.07	0.16
P5P(100 mM)	265.16	99.91
CoA(20 mM)	767.53	2264.21
ATP(100 mM)	551.14	315.53

Supplemental Table 2: Predicted optimal reaction mixtures from DOE models. Costs were calculated based substrates and cofactors required for each reaction. Reagent concentrations and costs are noted in supplemental table 1.

Predicted Optimal Number	Succinate(nL)	CoA(nL)	ATP(nL)	Glycine(nL)	P5P(nL)	Titer(mg/mL)	Cost/mg($)
Opt 1	25	0	15 0	400	42 5	0.038	5.91

			17		42		
Opt 2	0	0	5	400	5	0.048	5.09
			12		42		
Opt 3	50	0	5	400	5	0.052	3.96
			20		40		
Opt 4	0	0	0	400	0	0.06	4.31
					42		
Opt 5	100	0	75	400	5	0.056	2.96
			15		40		
Opt 6	25	0	0	425	0	0.05	4.36
			10		45		
Opt 7	100	0	0	350	0	0.052	3.68
					42		
Opt 8	125	0	50	400	5	0.054	2.68
					42		
Opt 9	175	0	25	375	5	0.052	2.42
					42		
Opt 10	175	0	0	400	5	0.045	2.39
Cost Opt					35		
1	225	0	0	425	0	0.05	1.76
Cost Opt					35		
2	200	0	0	450	0	0.054	1.62

Cost Opt 3	200	0	0	425	37 5	0.06	1.56
Cost Opt 4	250	0	0	475	27 5	0.049	1.41
Cost Opt 5	0	0	25	550	42 5	0.042	2.97
Cost Opt 6	0	0	0	575	42 5	0.041	2.62
Cost Opt 7	0	25	0	25	25	0	N/A
Cost Opt 8	0	0	0	525	0	0	N/A
Cost Opt 9	1000	0	0	0	0	0	N/A
Cost Opt 10	0	25	0	0	0	0	N/A
Base Reactio n	100	250	50	150	40 0	0.109	14.26

436 **Supplemental Table 3:** Plasmid sequence information for Hem pathway enzymes

Plasmid Name, accession number	Insert gene	Insert Sequence
mslpl004, pY71 HemA, Genbank MK	Hem A (*R. capsulatus)*	atggactacaatctcgcgctcgacaaagcgatccagaaactccacgacgagggacgttacc gcacgttcatcgacatcgaacgcgagaagggcgccttccccaaggcgcagtggaaccgcc ccgatggcggcaagcaggacatcaccgtctggtgcggcaacgactatctgggcatgggcca gcacccggtcgttctggccgcgatgcatgaggcgctggaagcggtcggggccggttcgggc ggcacccgcaacatctcgggcaccacggcctatcaccgccgtctggaagccgagatcgccg atctgcacggcaaggaagcggcgcttgtcttctcctcggcctatatcgccaatgacgcgacg ctctcgacgctgcggctgcttttccccggcctgatcatctattccgacagcctgaaccacgcct cgatgatcgaggggatcaagcacaatgccgggccgaagcggatcttccgtcacaatgacgt cgcccatctgcgcgagctgatcgccgctgatgatccggccgcgccgaagctgatcgccttcg aatcggtctattcgatggatggcgacttcggcccgatcaaggaaatctgcgacatcgccgat gaattcggcgcgctgacctatatcgacgaagtccatgccgtcggcatgtatggcccccgcgg cgcgggcgtggccgagcgtgacggtctgatgcaccgcatcgacatcttcaacggcacgctg gcgaaagcctatggcgtcttcggcggctacatcgccgcttcggcgaagatggtcgatgccgt gcgctcctatgcgccgggcttcatcttctcgacctcgctgccgccggcgatcgccgctggcgc gcaggcctcgatcgcgtttttgaaaaccgccgaagggcagaagctgcgcgacgcgcaaca gatgcacgcgaaggtgctgaaaatgcggctcaaggcgctggggatgccgatcatcgaccat ggcagccacatcgttccggtggtcatcggtgaccccgtgcacaccaaggcggtgtcggaca tgctcctgtcggattacggcgtttacgtgcagccgatcaacttcccgacggtgccgcgcggc accgaacggctgcgcttcacccccctcgccggtgcatgacctgaaacagatcgacgggctgg ttcatgccatggatctgctctgggcgcgctgtgcgtga
mslpl005, pY71 HemB	HemB (*E. coli*)	atgacagacttaatccaacgccctcgtcgcctgcgcaaatctcctgcgctgcgcgctatgttt gaagagacaacacttagccttaacgacctggtgttgccgatctttgttgaagaagaaattga cgactacaaagccgttgaagccatgccaggtgtgatgcgcattccagagaaacatctggca

		cgcgaaattgaacgcatcgccaacgccggtattcgttccgtgatgactttcggcatctctcac cataccgatgaaaccggcagcgatgcctggcgggaagatggactggtggcgcgaatgtcg cgcatctgcaagcagaccgtgccagaaatgatcgtcatgtcagacacctgcttctgcgaata cacatctcacggtcactgcggtgtgctgtgcgagcatggcgtcgacaacgacgcgactctgg aaaatttaggcaagcaagccgtggttgcagctgctgcaggcgcagacttcatcgccccttct gccgcgatggacggccaggtacaggcgattcgccaggcgctggacgctgcgggctttaaa gatacggcgattatgtcgtattcgaccaagttcgcctcttccttttatggtccgttccgtgaagc tgccggaagcgcattaaaaggcgaccgcaaaagctatcagatgaacccaatgaaccgtcg tgaggcgattcgtgagtcactgctggatgaagcccagggcgcagactgtctgatggttaaac ctgccggagcgtacctcgacatcgtgcgtgagctgcgtgaacgtactgaattgccgattggc gcgtatcaggtgagcggtgagtacgcgatgattaagttcgccgcgctggcgggtgctataga tgaagagaaagtcgtgctcgaaagcttaggttcaattaagcgtgcgggtgcggatctgatttt cagctactttgcgatggatttggctgagaagaagattctgcgttaa
mslpl006, pY71 HemC	HemC (*E. coli*)	atgttagacaatgttttaagaattgccacacgccaaagcccacttgcactctggcaggcaca ctatgtcaaagacaagttgatggcgagccatccgggcctggtcgttgaactggtaccgatgg tgacgcgcggcgatgtgattcttgatacgccgctggcgaaagtaggcggaaaaggcttattt gttaaagagctggaagtcgcgctcctcgaaaatcgcgccgatatcgccgtacattcaatgaa agatgtgccggttgaattcccgcaaggtctgggactggtcactatttgtgagcgtgaagatcc tcgcgatgcctttgtgtccaataactatgacaatctggatgcgttaccggcaggcagtatcgt cgggacgtccagtttacgtcgccagtgccaactggctgaacgccgcccggatctgattatcc gctccctgcgaggcaacgtcggcactcgcctgagtaaactggataacggcgaatacgatgc catcattcttgcggtagccggactaaaacgtttaggtctggagtcccgcattcgcgccgcatt gccacccgagatttctcttccggcggtaggacaaggtgcggtgggtattgaatgccgccttg atgattctcgcactcgcgagctgcttgccgcgctgaatcaccacgaaactgcactgcgcgtta ccgcagaacgcgccatgaatacccgtctcgaaggcggatgtcaggtgccaattggtagcta cgccgagcttattgatggcgaaatctggctgcgtgcgttggtcggcgcgccggacggttcgc

		agattattcgcggtgaacgccgcggtgcgccgcaagatgccgaacaaatggggatttcgct ggcagaagagctactgaataacggcgcgcgcgagatcctcgctgaagtctataacggaga cgctccggcatga
mslpl007, pY71 HemD	HemD (*E. coli*)	atgagtatccttgtcacccgcccgtctcccgctggagaagagttagtgagccgtctgcgcac actggggcaggtggcctggcattttccactgattgagttttctccgggtcgacaattaccaca acttgctgatcaactggcggcgctgggggagagcgatctgttgtttgccctctcgcaacacg cggttgcttttgcccaatcacagctgcatcagcaagatcgtaaatggccccgactacctgatt atttcgccattggacgcaccaccgcactggcactacataccgtaagcggacagaagattctc tacccgcaggatcgggaaatcagcgaagtcttgctacaattacctgaattacaaaatattgc gggcaaacgtgcgctgatattacgtggcaatggcggtcgtgagctaattggggataccctga cggcgcgcggtgctgaggtcacttttgtgaatgttatcaacgatgcgcaatccattacgatg gtgcagaagaagcgatgcgctggcaatcccgcgaggtgacgacggtcgttgttaccagcgg tgaaatgttgcagcaactctggtcgctgatcccacaatggtatcgtgagcactggttactaca ctgtcgactattggtcgtcagtgagcgtttggcgaaactcgcccgggaactgggctggcaag acattaaggtcgccgataacgctgacaacgatgcgcttttacgggcattacaataa
mslpl008, pY71 HemE	HemE (*E. coli*)	atgaccgaacttaaaaacgatcgttatctgcgggcgctgctgcgccagcccgttgatgtcact ccagtatggatgatgcgccaggcgggtcgctatctaccggaatataaagccacgcgcgccc aggccggcgattttatgtcgctgtgcaaaaacgccgagctggcgtgcgaagtgactttgcaa ccgctgcgtcgctacccgctggatgcggcgatcctcttttccgatatcctcaccgtgccggac gcgatggggttagggctctattttgaagccggagaaggtccgcgttttacctcgccagtcacc tgcaaagccgacgtcgataaactgccaattccggacccggaagatgagctgggttacgtga tgaacgcggtgcgtaccattcgtcgcgaactgaaaggcgaagtgccgctgattggtttttcc ggcagcccgtggacgctggcgacctacatggtggaaggcggcagcagcaaagcgttcacc gtgatcaaaaaaatgatgtatgccgatccgcaggcgctgcacgctctactcgataaactggc gaaaagcgtcactttgtatctgaatgcgcagattaaagtcggtgctcaggcagtgatgatttt cgacacctggggcggcgtgcttaccgggcgcgattatcaacagttctcgctctattacatgca

		taaaattgttgatggtttactgcgtgaaaacgacggtcgccgcgtaccggtcacgctgtttac caaaggcggcggacagtggctggaagcgatggcagaaaccggttgcgatgcgcggggcct cgactggacaacggacatcgccgatgcgcgccgccgtgtgggcaataaagtcgcgttgcag ggtaatatggatccgtcgatgctgtacgcgccgcctgcccgcattgaagaagaagtagcga ctatacttgcaggtttcggtcacggcgaaggtcatgtctttaaccttggtcacggcattcatca ggatgtgccgccagaacatgctggcgtgttcgtggaggcagtgcatcgactgtctgaacagt atcaccgctaa
mslpl009, pY71 HemF	HemF (*E. coli*)	atgaaacccgacgcacaccaggttaaacagtttctgctcaaccttcaggatacgatttgtca gcagctgaccgccgtcgatggcgcagaatttgtcgaagatagttggcagcgcgaagctggc ggcggcgggcgtagtcgggtgttgcgtaatggtggtgttttcgaacaggcaggcgtcaactt ttcgcatgtccacggtgaggcgatgcctgcttccgccaccgctcatcgcccggaacttgccg ggcgcagtttcgaggcgatgggcgtttcactggtagtgcatccgcataacccgtatgttccca ccagccacgcgaatgtgcggtttttattgccgaaaaaccgggtgccgatcccgtctggtggt ttggcggcggcttcgatttaaccccttttctatggttttgaagaagacgccattcactggcaccg caccgcccgtgacctgtgcctgccatttggtgaagacgtttatccccgttacaaaaagtggtg cgacgattacttctacctcaaacatcgcaacgaacagcgcggtattggcgggctgttctttga tgatctgaacacgccagatttcgaccactgttttgcctttatgcaggcggtaggcaaaggcta caccgacgcttatttaccaattgtagagcgacgtaaagcgatggcctacggcgagcgcgag cgcaattttcagctctaccgtcgcggtcgttatgtcgagttcaatctggtctgggatcgcggca cgctgtttggcctgcaaactggcgggcgcaccgagtctatcctgatgtcaatgccgccactg gtacgctgggaatatgattatcagccaaaagatggcagcccagaagcggcgttaagtgagt ttattaaggtcagggattgggtgtaa
DG186, pTwist High Copy HemG	HemG (*E. coli*)	atgaaaaccctgatactgttttcaacacgcgatggccagacccgggaaattgcgtcatatct cgcgtccgaactgaaagagctgggtattcaggctgacgttgcgaacgttcatcgtatagaag aaccacagtgggaaaattatgatcgtgtcgtaataggagcttcgatccggtatggacattat cacagcgccttccaggaattcgtcaaaaaacacgcgactagactgaacagcatgccgtccg

		cattctactcggttaaccttgtagcccgcaagcctgaaaaaagaacaccgcagaccaatag ctatgctcgtaaattcctgatgaactcgcagtggcgtcccgatcgctgcgccgttattgcggg tgcattgcgctatcctcgttatcgttggtatgatcgctttatgatcaaactgatcatgaaaatgt ctggcggtgagacagatacgagaaaagaggtagtatatactgattgggaacaggttgcaa atttcgctcgtgaaattgcgcacttgaccgacaaaccgacattaaaataa

437